Ruthenium(II) complexes of 6-hydroxydipyrido[3,2-*a*:2′,3′-*c*]phenazine: self-association, and concentration-dependent acid–base and DNA-binding properties†

Mei-Jiao Han, Yan-Min Chen and Ke-Zhi Wang*

Received (in Montpellier, France) 1st August 2007, Accepted 14th January 2008
First published as an Advance Article on the web 11th February 2008
DOI: 10.1039/b711759k

6-Hydroxydipyrido[3,2-*a*:2′,3′-*c*]phenazine (hdppz) and its ruthenium(II) complexes of $[Ru(bpy)_2(hdppz)]X_2$ (bpy = 2,2′-bipyridine and X = ClO_4^-, PF_6^- and Cl^-) have been synthesized and characterized. The ion association (self aggregation of the complex cation, and ion pairing) behaviors have been studied in both aqueous and nonaqueous (MeCN) media by UV-visible spectrophotometric measurements. The concentration-dependent ground- and excited-state acid–base properties of the perchlorate complex have been studied by pH spectrophotometric titrations. Calf thymus DNA binding properties of the perchlorate complex have been studied by UV-visible and luminescence titrations, steady-state emission quenching by $[Fe(CN)_6]^{4-}$, DNA competitive binding with ethidium bromide, DNA melting experiments, and viscosity measurements. The results have shown that the ion association properties are markedly influenced by the counter ions and concentrations with the effects of ClO_4^- being the most prominent. The ion association in aqueous solution for the perchlorate complex moderately affects acidity ionization constants of the complex by a difference of over 0.2 pH units, but affects DNA binding constants significantly by a difference of over one order of magnitude, as studied at two $[Ru(bpy)_2(hdppz)](ClO_4)_2$ concentrations of 4 and 20 μM. $[Ru(bpy)_2(hdppz)](ClO_4)_2$ was demonstrated to act as a DNA intercalator and a rare "turn-on" type pH emission molecular switch driven by the deprotonation of the hydroxy group over the pH range 6.00–11.50 with an emission enhancement factor of 150.

1 Introduction

The development of luminescent signaling devices is an active area of supramolecular chemistry. The molecules whose emissions are modulated by single or several external sources such as light, ions, pH, and biomolecules, are of particular interest,[1a–e] can serve as intriguing luminescent switches, sensors, and logic gates.[1d–h] Polypyridyl ruthenium complexes are ideally suited for applications as sensitive optical sensors and probes,[2] because they have intriguing ground- and excited-state photophysical, photochemical and redox properties, and are inert to substitution. Among them dipyridophenazine complexes of ruthenium(II) have shown interesting properties that could be used for the development of sensors of high sensitivity and selectivity. The complex $[Ru(phen)_2(dppz)]^{2+}$ and its cousin $[Ru(bpy)_2(dppz)]^{2+}$ (bpy = 2,2′-bipyridine, phen = 1,10-phenanthroline, dppz = dipyrido[3,2-*a*:2′,3′-*c*]phenazine) have the metal-to-ligand-charge-transfer (MLCT) states which are localized on the electron-withdrawing dppz ligand. These molecules show negligible photoluminescence at ~610 nm in aqueous solution at ambient temperatures but emit brightly in non-aqueous solutions such as acetonitrile or alcohol.[3] The photophysical properties of these molecules can be theoretically explained.[4] Biomolecules such as DNA, can also provide local non-aqueous pockets for these complexes, and hence, luminescence is observed in these systems. Luminescence enhancements by a factor of over 10^4 are estimated upon binding of $[Ru(phen)_2(dppz)]^{2+}$ to DNA.[5] Accumulated evidence points to hydrogen bonding and/or excited-state proton transfer to the phenazine nitrogens as the mechanism of deactivation of the complex's excited state.[5,6] Polypyridyl Ru(II) complexes can bind to DNA in non-covalent binding fashions of electrostatic, groove and intercalative including classical intercalation, semi-intercalation and quasi-intercalation.[7] Many important applications of these complexes require that the complex binds to DNA through an intercalative mode. The factors influencing the DNA binding affinity and selectivity also arose intensive efforts. The shape and planarity of the main ligand[7,8] is thought to play a key role in binding mode and affinity, also ancillary ligand[9] can directly or indirectly affect the DNA binding properties through changing the planarity of the main ligand, and the hydrophobicity of the complex. All the studies indicated that a subtle change in the molecular structure may exert significant effects on binding

College of Chemistry, Beijing Normal University, Beijing 100875, China. E-mail: kzwang@bnu.edu.cn; Fax: +86-10-58802075; Tel: +86-10-58805476/62209940

† Electronic supplementary information (ESI) available: Concentration-dependent UV-visible spectra for $[Ru(bpy)_2(hdppz)]X_2$ (X = PF_6 and Cl) in aqueous solution, and for $[Ru(bpy)_2(dppz)]X_2$ (X = PF_6 and Cl) in both aqueous and MeCN solutions, and the changes in UV-visible spectra of $[Ru(bpy)_2(hdppz)]Cl_2$ in MeCN at 0.63 μM and 17.6 μM with increasing concentrations of $NaClO_4$ (0.1–1.0 M). See DOI: 10.1039/b711759k

modes, locations, and affinities, and provide a chance to explore various valuable information regarding conformation- or site-specific DNA probes.

On the other hand, the pH responsive transition-metal complexes containing *N*-heterocyclic ligands are one family of fundamental molecular devices with adjustable ground- and excited-state properties.[10] Many life processes, such as enzymes, operate within a very narrow pH window, where their function or activity can be described as being "*switched on*" or "*switched off*" as a function of pH.[11a] Attempts to mimic such "*off–on–off*" or "*on–off–on*" behaviour by constructing luminescence devices that are modulated by pH have recently been achieved by employing Ru(II) complexes,[10] but, more work are required to broaden pH windows, and to improve the sensitivity of pH responses. Also, the Ru(II) complex-based interesting pH-dependent DNA damage and selectivity towards cancer cells have recently been demonstrated.[11b]

Many Ru(II) complexes like that we studied in this paper, are ionic and are of planar conjugation system, and so two types of associations in fluid solution are possible: one is the association of the ruthenium complex cations *via* π–π stacking or/and intermolecular H-bonding interaction (self aggregation),[12] and the other is the association of the Ru(II) complex cation with their respective counter anion (the formation of ion pairs).[13] Several Ru(II) complexes were evidenced by concentration-dependent ^{1}H NMR spectra or single-crystal X-ray structures to exist in solutions or in the solid as dimers,[12] which are ascribed to self-aggregation *via* intermolecular π–π stacking of their aromatic chromophores.[12] The ionic complexes were reported to exist in solutions of usually low relative permittivity as not simply solvated species but as ion pairs, as discussed in two recent reviews.[13b,c] Some Ru(II) cationic complexes were reported to form ion pairs even in medium-polarity solvents such as ethanol and methanol,[14,15] even higher aggregates such as quadruples in such favourable conditions as increased concentration in solvents with low relative permittivity, and facilitation by "inter-ion-pair" hydrogen bonding or π–π stacking interactions.[15] Ion-pairing can affect both the thermodynamics of a reaction, by changing the relative energies of the reagents and the products, and its kinetics, mechanism, reaction activity and selectivity particularly markedly by providing alternative reaction pathways.[14,15] However, little is known about the effects of the two association properties mentioned above for Ru(II) complexes on their acid–base and DNA binding properties.

Recently, we have reported acid–base, DNA molecular light switching, and DNA binding properties of a series of structurally related polypyridyl Ru(II) complexes.[16] The large luminescence on–off ratios on basis of the Ru(II) complexes induced by pH changes over both acidic and basic pH ranges,[16a,b] and by DNA binding[16c,i] have been achieved by us. We have also found that the self aggregation of $[Ru(bpy)_2(dppz)](ClO_4)_2$ markedly affects its DNA binding properties.[16j] In order to gain more insights into the two types of association behaviors (self aggregation and ion pairing) of Ru(II) polypyridyl complexes, and how these association behaviors affect DNA binding and acid–base properties, we have synthesized three $[Ru(bpy)_2(dppz)]^{2+}$ analogous complexes of $[Ru(bpy)_2(hdppz)]X_2$ (hdppz = 6-hydroxydipyrido-[3,2-*a*:2′,3′-*c*]phenazine, X = ClO_4^-, PF_6^- and Cl^-) with variations of the counter anions. The molecular structure of $[Ru(bpy)_2(hdppz)]^{2+}$ is shown in Scheme 1. We have also demonstrated in this paper that $[Ru(bpy)_2(hdppz)]^{2+}$ acts as both a calf thymus DNA intercalator, and a rare "turn-on" type emission molecular switch with a large on–off ratio of 150 driven by deprotonation of the hydroxy group.

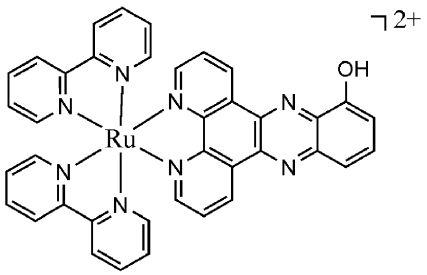

Scheme 1 Molecular structure of $[Ru(bpy)_2(hdppz)]^{2+}$.

2 Experimental

2.1 Physical measurements

Infrared spectra were recorded with a Nicolet Avtar 360FT-IR spectrometer as KBr disks. ^{1}H NMR spectra were collected with a Bruker DRX-500 NMR spectrometer with $(CD_3)_2SO$ as solvent at room temperature. Microanalyses (C, N and H) were performed with a Vario EL elemental analyzer. UV-visible absorption spectra were recorded with a GBC Cintra 10e UV-visible spectrophotometer. Emission spectra were obtained on a Shimadzu RF-5301PC spectrofluorimeter. The emission quantum yields were calculated by comparison with $[Ru(bpy)_3]^{2+}$ (φ_{std} = 0.028)[17] in aerated aqueous solution at room temperature using eqn (1):

$$\varphi = \varphi_{std}(A_{std}/A)(I/I_{std}) \quad (1)$$

where φ and φ_{std} are the quantum yields of unknown and the standard samples; A and A_{std} are the absorbances at the excitation wavelength; I and I_{std} are the integrated emission intensities. UV-visible and emission spectrophotometric pH titrations were carried out in aqueous solutions containing a Britton–Robinson (BR) buffer and 0.2 M NaCl to keep a constant ionic strength.

All experiments dealing with the interaction of Ru(II) complexes with calf thymus DNA (ct-DNA) were carried out in 5 mM Tris–HCl buffer (pH 7.1, 50 mM NaCl). Steady-state emission quenching experiments were carried out in Tris–HCl buffer by using $[Fe(CN)_6]^{4-}$ as the quencher. The experiments of DNA thermal denaturation were performed on UV-visible spectrophotometer in a buffer consisting of 1.5 mM Na_2HPO_4, 0.5 mM NaH_2PO_4 and 0.25 mM Na_2EDTA. Viscosity measurements were carried out using an Ubbelodhe viscometer maintained at a constant temperature at 32.10 ± 0.02 °C in a thermostatic bath. Flow time was measured and each sample was measured at least three times, and an average flow time was calculated. Data were presented as $(\eta/\eta_0)^{1/3}$ *vs.* [Ru]/[DNA], where η is the viscosity of DNA in the presence of the Ru complex and η_0 is the viscosity of DNA alone.

2.2 Synthesis

2.2.1 Preparation of 6-hydroxydipyrido[3,2-*a*:2′,3′-*c*]phenazine (hdppz). The ligand hdppz was synthesized *via* a modification of the literature method.[18a] 1,10-Phenanthroline-5,6-dione[18b] (0.210 g, 1 mmol) was added to a boiling solution of 2,3-diaminophenol (0.124 g, 1 mmol) in ethanol. The reaction mixture was refluxed for 6 h, then filtered while hot. After most of the solvent was removed under reduced pressure, a yellow power was obtained. The crude product was then recrystallized twice from MeOH. Yield: 0.137 g, 45.9%. IR: ν_{max} (KBr, cm^{-1}) 3453vs, 1580m, 1489m, 1422m, 1354vs, 742vs. ^{1}H NMR (500 MHz, DMSO-d_6): δ/ppm 10.71 (s, 1H), 9.93 (d, 1H, J = 8.0), 9.50 (d, 1H, J = 8.1), 9.20 (m, 2H), 7.94 (m, 2H), 7.91 (t, 1H, J = 7.8), 7.82 (d, 1H, J = 8.5), 7.34 (d, 1H, J = 7.5).

2.2.2 Preparation of $[Ru(bpy)_2(hdppz)](ClO_4)_2{\cdot}2H_2O$. A suspension of $[Ru(bpy)_2Cl_2]{\cdot}2H_2O$[19] (0.104 g, 2 mmol) and hdppz (0.060 g, 2 mmol) in 75 mL EtOH–H_2O (v/v, 2 : 1) was refluxed under nitrogen for 10 h. After most of the solvent was removed under reduced pressure, a red precipitate was obtained by dropwise addition of 4-fold excess of saturated aqueous $NaClO_4$ solution. The crude product was then recrystallized by diffusion of diethyl ether vapour into a concentrated acetonitrile solution of the complex. Yield: 0.181 g, 94.5%. IR: ν_{max} (KBr, cm^{-1}) 3418vs, 1590s, 1121vs, 1090vs (ClO_4^-). Anal. Calc. for $C_{38}H_{26}N_8\ Cl_2O_9Ru{\cdot}2H_2O$: C, 48.21; H, 3.19; N, 11.84. Found: C, 48.4; H, 3.09; N, 11.38%. ^{1}H NMR (500 MHz, DMSO-d_6): δ/ppm 10.00 (d, 1H, J = 8.2), 9.61 (d, 1H, J = 8.2), 8.87 (d, 2H, J = 8.2), 8.84 (d, 2H, J = 8.2), 8.20 (m, 4H), 8.14 (t, 2H, J = 7.9), 8.02 (m, 3H), 7.96 (d, 1H, J = 8.0), 7.84 (d, 2H, J = 5.3), 7.78 (t, 2H, J = 3.8), 7.60 (t, 2H, J = 6.4), 7.39 (d, 1H, J = 5.3), 7.38 (m, 2H).

2.2.3 Preparation of $[Ru(bpy)_2(hdppz)]Cl_2{\cdot}5H_2O$. This chloride salt was prepared from the perchlorate by precipitation in acetone solution with tetra-*n*-butylammonium chloride and recrystallized from MeCN–H_2O–Et_2O. IR: ν_{max} (KBr, cm^{-1}) 3423vs, 1632s, 1444m, 1421s, 768vs. Anal. Calc. for $C_{38}H_{26}N_8Cl_2ORu{\cdot}5H_2O$ (%): C, 52.30; H, 4.16; N, 12.84. Found: C, 52.55; H, 4.59; N, 12.93.

2.2.4 Preparation of $[Ru(bpy)_2(hdppz)](PF_6)_2{\cdot}2H_2O$. The complex was prepared and purified by the same procedure described above except for that NH_4PF_6 was used instead of $NaClO_4$. IR: ν_{max} (KBr, cm^{-1}) 3438vs, 1629s, 1446s, 841vs (PF_6^-). Anal. Calc. for $C_{38}H_{26}N_8Cl_2F_{12}OP_2Ru{\cdot}2H_2O$ (%): C, 44.03; H, 3.04; N, 10.98. Found: C, 43.98; H, 2.91; N, 10.80.

3 Results and discussion

3.1 Self-association of the Ru(II) complexes

The many literature studies[12] on Ru(II) complexes by means of NMR spectroscopy for solutions and crystal structural studies for solids[12h,i] have provided evidence that despite the electrostatic repulsion between ruthenium(II) complex cations, H-bonding and π–π stacking interaction allow the complexes themselves to tightly self-associate. On the other hand, the formation of ion pairs between oppositely charged Ru(II) complex cation and counter anion are receiving increasing attention due to its profound effects on reaction dynamics and mechanism, in spite of its weak electrostatic interaction with respect to strong π–π and H-bonding interactions. Although NMR spectroscopy is proven to be a popular technique for the study of association properties of Ru(II) complexes in solutions, this technique usually used concentrations of the complexes as high as >1 mM. In fact, some Ru(II) complexes would start to aggregate at much lower concentrations than those used for NMR studies. We have recently successfully observed evident aggregation of $[Ru(phen)_2(dppz)](ClO_4)_2$ at concentrations C_{Ru} >0.3 μM by UV-visible spectroscopy.[16j] Since concentrations, counter ions and solvents were reported to influence the self aggregation and ion pairing of Ru(II) complexes, we have studied concentration-dependent UV-visible spectra of three complexes of $[Ru(bpy)_2(hdppz)]X_2$ with variations of counter anions in both 5 mM Tris–HCl buffer (pH 7.1, 50 mM NaCl) aqueous and non-aqueous (MeCN) media. The changes in the apparent molar extinction coefficients (ε) upon increasing total concentrations of $[Ru(bpy)_2(hdppz)](ClO_4)_2$ in Tris–HCl buffer and MeCN are compared in Fig. 1. The UV-visible spectrum of

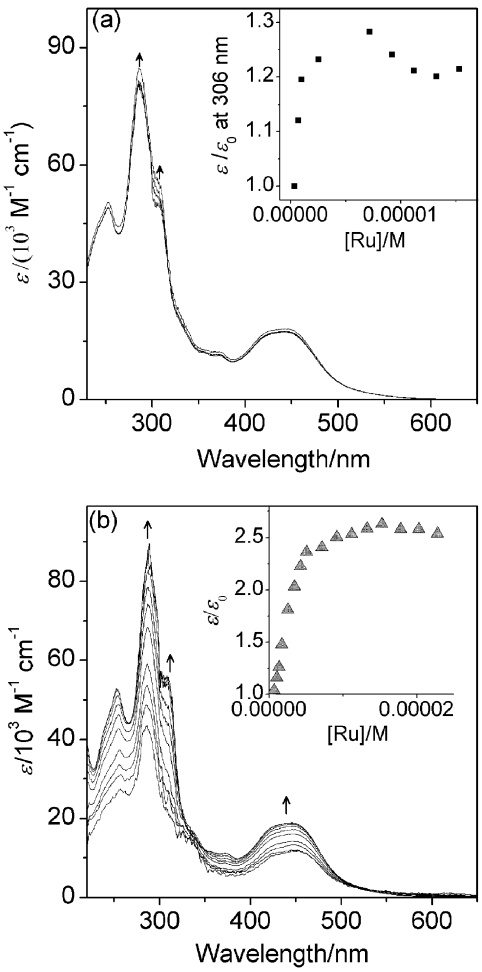

Fig. 1 The changes in UV-visible spectra upon increasing the concentrations (0–25.0 μM) of $[Ru(bpy)_2(hdppz)](ClO_4)_2$ in 5 mM Tris–HCl buffer (50 mM NaCl) aqueous solution at pH = 7.0 (a), and in MeCN (b). Inset: plots of $\varepsilon/\varepsilon_0$ *vs.* [Ru].

$[Ru(bpy)_2(hdppz)](ClO_4)_2$ in Tris–HCl aqueous solution mainly consists of four well-resolved bands at 253, 287, 305 and 443 nm. The former two bands are attributed to the $\pi \rightarrow \pi^*$ (bpy) transitions, the third UV band to $\pi \rightarrow \pi^*$ (hdppz) intraligand (IL) transition, and lowest-energy band at 443 nm is assigned to a mixture of MLCT transitions of $Ru(d\pi) \rightarrow$ hdppz(π^*) and $Ru(d\pi) \rightarrow$ bpy (π^*) by analogy to the parent $Ru(bpy)_3^{2+}$ and analogous polypyridyl dppz Ru(II) complexes.[20] In the concentration range (0.3–7.0 μM) of the complex, ε values at 305 nm increase with increasing concentrations of the complex, indicating that aggregation or ion pairing reaction would be occurring, although we would not detect minimum Ru(II) complex concentration due to instrumental detection limitation. At $[Ru(bpy)_2(hdppz)](ClO_4)_2$ concentrations higher than 7.0 μM, the ε values at 305 nm remain almost unchanged (see the inset of Fig. 1), suggesting that the association reaction has finished. Although the spectral changes shown in Fig. 1 for $[Ru(bpy)_2(hdppz)](ClO_4)_2$ in Tris–HCl aqueous solution are not very large, they are more apparent than those observed for $[Ru(bpy)_2(hdppz)](PF_6)_2$ and $[Ru(bpy)_2(hdppz)]Cl_2$ in the same medium (see ESI†), indicative of strong dependence of the association properties of the complexes on the counter ions. As shown in Fig. 1(b), the spectral changes in MeCN for $[Ru(bpy)_2(hdppz)](ClO_4)_2$ are much more evident than in Tris–HCl buffer, with ε values at 253, 287, 308 and 443 nm dramatically increasing, and an isosbestic point appearing at 342 nm over Ru(II) concentrations 0.3 μM < [Ru] < 5.0 μM, indicating that aggregation or ion pairing reaction of the complex occurs over this concentration range. As anticipated, the spectral changes in MeCN are also dependent on the counter ions with the complexes of both Cl^- and PF_6^- counter ions (see ESI†) being less evident than that observed for $[Ru(bpy)_2(hdppz)](ClO_4)_2$ in the same solvent. Similarly, the spectral changes upon increasing concentrations of $[Ru(bpy)_2(dppz)](ClO_4)_2$ in MeCN are much more striking than those observed for $[Ru(bpy)_2(dppz)]Cl_2$ in the same solvent (see ESI†). In order to ascertain the role played for the spectral changes in Fig. 1(b) by self aggregation of the complex cation, and ion pairing between $[Ru(bpy)_2(hdppz)]^{2+}$ and ClO_4^-, we have carried out experiments of the effects of varied concentrations of $NaClO_4$ on the UV-visible spectra of $[Ru(bpy)_2(hdppz)]Cl_2$ in MeCN (see ESI†). Successive addition of $NaClO_4$ (0.1–1.0 M) to a MeCN solution of $[Ru(bpy)_2(hdppz)]Cl_2$ at a low concentration of 0.625 μM at which the complex would be reasonably supposed to exist dominantly as a monomer, results in marked spectral changes with intensities for the bands at 251, 289, 306, 368 and 436 nm increasing in a way similar to those observed for concentration-dependent UV-visible spectra in MeCN (Fig. 1(b)), in which the much larger hyperchromicity in intensities for the band at 368 nm is observed, and isosbestic point experiences a blue shift to 318 nm relative to a value of 342 nm observed in Fig. 1(b). If ion pairs in solution were dominant relative to self-aggregated species of the complex cation, addition of high concentrations of $NaClO_4$ to a MeCN solution of high concentration of $[Ru(bpy)_2(hdppz)]Cl_2$ should evidently alter the equilibrium state of ClO_4^--involved ion pair formation reaction, and thus the UV-visible absorption spectra of $[Ru(bpy)_2(hdppz)]Cl_2$ in MeCN. On the contrary, successive addition of $NaClO_4$ to a MeCN solution of $[Ru(bpy)_2(hdppz)]Cl_2$ at a high concentration of 17.65 μM only slightly altered the UV-visible spectra of $[Ru(bpy)_2(hdppz)]Cl_2$, in a way similar to those observed for concentration-dependent UV-visible spectra of two complexes of $[Ru(bpy)_2(hdppz)](PF_6)_2$ and $[Ru(bpy)_2(hdppz)]Cl_2$ in Tris–HCl buffer. It was reported that ion pairing is favored by solvents of low or medium relative permittivity such as MeCN, and addition of high concentrations of $NaClO_4$ should promote ion pairing more than ion-induced complex cation aggregation. The above results led us to make a conclusion that the evident spectral changes observed in Fig. 1(b) are dominantly contributed by ion pairing rather than the self aggregation of the complex cation, while the spectral changes shown in Fig. 1(a) for concentration-dependent UV-visible spectra of $[Ru(bpy)_2(hdppz)](ClO_4)_2$ in Tris–HCl buffer are mainly due to the aggregation of the complex cation $[Ru(bpy)_2(hdppz)]^{2+}$, although in both cases self aggregation of the complex cation, and ion pairing most probably come into play simultaneously. Apparently, the more evident spectral changes observed for $[Ru(bpy)_2(hdppz)](ClO_4)_2$ in MeCN than those observed for $[Ru(bpy)_2(dppz)](ClO_4)_2$ in the same solvent are due to the presence of the hydroxy group on hdppz, although the role played by the hydroxy group is unclear at the present time.

In order to derive the aggregation constant of $[Ru(bpy)_2(hdppz)](ClO_4)_2$ in Tris–HCl buffer, we assume that self aggregation of $[Ru(bpy)_2(hdppz)]^{2+}$ results in only the dimer and no higher order oligomers under our experimental conditions. The dimerization constant K_D and the molar extinction coefficient of the dimer ε_D can be obtained[21] from the eqn (2):

$$\sqrt{\frac{\varepsilon - \varepsilon_M}{C_M^0}} = \sqrt{\frac{2K_D}{\Delta\varepsilon}}(\Delta\varepsilon - (\varepsilon - \varepsilon_M)) \qquad (2)$$

where ε, ε_M and ε_D are the extinction coefficients of the solution, the pure monomer, and the pure dimer, respectively, $C_M{}^0$ is the total concentration of the complex, and $\Delta\varepsilon = \varepsilon_D - \varepsilon_M$. Accordingly a plot of $[(\varepsilon - \varepsilon_M)/C_M{}^0]^{1/2}$ *versus* $(\varepsilon - \varepsilon_M)$ should yield a straight line with the intercepts $(2K_d\Delta\varepsilon)^{1/2}$ (on the ordinate axis) and $\Delta\varepsilon$ (on the abscissa axis). By substituting $\varepsilon_M = 4.3 \times 10^4\ M^{-1}\ cm^{-1}$ in water, a K_D values of $(4.4 \pm 0.4) \times 10^3\ M^{-1}$, and an ε_D values of $4.5 \times 10^4\ M^{-1}$ at 306 nm were derived for $[Ru(bpy)_2(hdppz)](ClO_4)_2$ in Tris–HCl buffer.

3.2 The pH effects on UV-visible and emission spectra

3.2.1 UV-visible spectra and the ground-state pK_a. Since the association of the complex in aqueous solution is concentration-dependent, and may affect the acid–base properties of $[Ru(bpy)_2(hdppz)](ClO_4)_2$, UV-visible spectrophotometric pH titrations were carried out over the pH range 1.00–13.00 at two concentrations of the complex, one concentration is 1.50 μM at which the complex was assumed to be dominantly monomeric, and the other concentration is 15.4 μM at which the complex fully dimerizes. The changes in the UV-visible absorption spectra for $[Ru(bpy)_2(hdppz)](ClO_4)_2$ at the concentration of 15.4 μM in BR buffer as a function of pH are shown in Fig. 2(a). As the pHs of aqueous $[Ru(bpy)_2(hdppz)](ClO_4)_2$ were raised over the pH range above mentioned, the lowest-

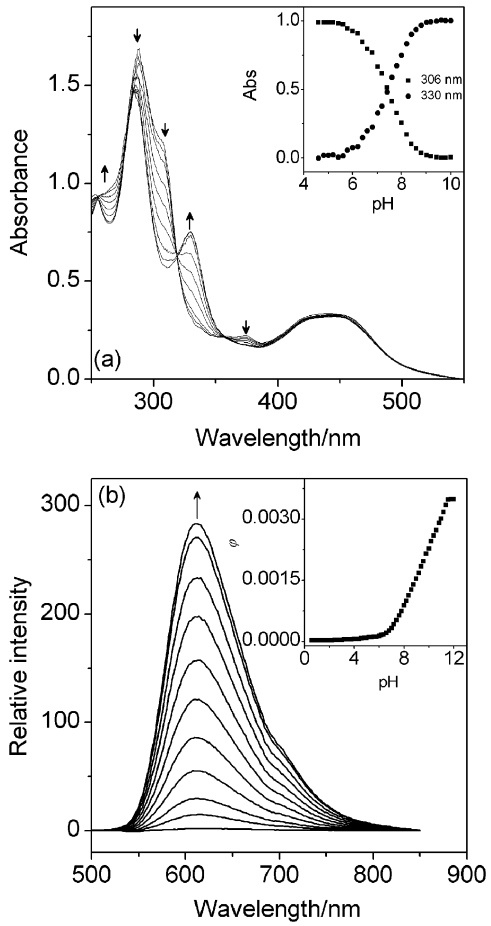

Fig. 2 pH effects on the UV-visible spectra (a) and emission (λ_{ex} = 460 nm) spectra (b) of $[Ru(bpy)_2(hdppz)](ClO_4)_2$ (15.4 μM) in a Britton–Robinson buffer (0.2 M NaCl). Arrows show spectral changes upon increasing pH from 6.00 to 11.50.

energy MLCT band kept its maximum and intensities almost unchanged at ~443 nm. However, as pHs were further increased from 6.0 to 9.0, the high-energy band at 305 nm, owing to the intraligand π → π* (hdppz) transition, decreased considerably in the intensities, a new band centering at 330 nm appeared, and the intensities of π → π* bands at 287 and 374 nm were moderately reduced, resulting in three isosbestic points occurring at 317, 360 and 386 nm, respectively, accompanying with a blue-shift by 5 nm for the band at 287 nm. The presence of isosbestic points verified the existence of two detectable species in the equilibrium, that is, the deprotonated and fully protonated forms. The spectral changes observed here are due to the dissociation of the proton on the hydroxy moiety obviously. The new band at 330 nm was assigned to the π → π* transition of deprotonated hdppz. Titration curves, obtained by plotting the changes in absorbance at 327 and 305 nm *vs.* pH are shown in the insets of Fig. 2(a). Similar spectral changes were observed for the complex at the concentration of 1.50 μM (Figure not shown). The ground-state ionization constants were derived to be $pK_a = 7.20 \pm 0.01$ and 7.40 ± 0.01 for the complex at concentrations of 1.50 and 15.4 μM, respectively, by nonlinear sigmoidal fit of the data in the insets of Fig. 2(a), and were compared with the pK_a values for hydroxy-containing Ru(II) complexes in Table 1. The pK_a values (7.20–7.40) observed for $[Ru(bpy)_2(hdppz)]^{2+}$ at the two concentrations mentioned above are more acidic than pK_a ~ 10.0 reported for $[Ru(L)_2(dhphen)]^{2+}$ (dhphen = 4,7-dihydroxy-1,10-phenanthroline, L = 2,2′-bipyridine or 1,10-phenanthroline or 3,4,7,8-tetramethyl-1,10-phenanthroline),[22] $pK_a = 8.6$ reported for $[Ru(bpy)_2(hpbpy)]^{2+}$ (hpbpy = 4-(4-hydroxyphenyl)-2,2′-bipyridine),[23a] due mainly to the fact that hdppz is more conjugated than dpphen and hpbpy. However, the pK_a values of 7.20–7.40 are more basic than hydroxy-deprotonated pK_a of 6.0 (the first hydroxy) for $[Ru(bpy)_2dpq(OH)_2]^{2+}$, and 6.4 for $[Ru(bpy)_2dpqOHCOOH]^{2+}$,[23b] due to intra-molecular H-bonding effects.[24]

3.2.2 Luminescence spectra and the excited state pK_a*. The emission spectra of $[Ru(bpy)_2(hdppz)](ClO_4)_2$ were strongly pH dependent as shown in Fig. 2(b). The emission intensities *vs.* pH profile shown in the inset of Fig. 2(b), was composed of only one sigmoidal curve which were due to the excited-state protonation/deprotonation processes of the hydroxy group over pH region from 6.00 to 11.5. In acidic solutions of pH below 6.00, where the deprotonation of the hydroxy moiety in the complex does not occur, the complex emits weakly with luminescence peak at 619 nm (λ_{ex} = 460 nm, φ = 0.029%), which is characteristic of ^{3}MLCT (dπ(Ru) → dπ*(ligand)) emission state.[25] The emission intensities were found to increase sharply upon increasing pH from 6.00 to 11.5 with the emission maxima blue-shifting from 619 nm to 611 nm. Over this pH region the complex acts as an 'off–on' emission switch with an on/off ratio of more than 150. Similar behavior was observed for the complex at low concentration of 1.50 μM. This emission enhancement factor is the largest value among those previously reported for representative pH sensors of Ru(II) complexes operated over the basic pH range (see Table 1).[16a,b,d,23,26] Obviously, emission switching observed on $[Ru(bpy)_2(hdppz)]^{2+}$ is operated by much increased non-radiative decay routes rather than a photoinduced electron transfer mechanism from a strong electron donor, deprotonated hydroxy, to the excited Ru(II) complex. The excited-state ionization constant pK_a* could be derived in two ways, one is an accurate assessment based on the equation: $pK_a^* = pH_i + \log(\tau_{HB}/\tau_B)$,[10a] where pH_i is a reflection point obtained from the emission titration curve, τ_{HB} and τ_B are the emission lifetimes of the protonated and deprotonated species, respectively. From the above equation, we can see that if pK_a* were greater than pK_a, it would result in that the pH regions for causing UV-visible and emission spectral changes are different. Even if pK_a approximately equals pK_a*, different τ_{HB} and τ_B can also lead to the inconsistency in pH ranges for UV-visible and emission spectral changes. The pH range 6.00–11.5 observed for $[Ru(bpy)_2(hdppz)](ClO_4)_2$ in emission spectrophotometric titrations is more basic than pH = 6.00–9.00 observed in UV-visible spectrophotometric titrations, which is common for Ru(II) polypyridyl complexes reported,[10a] *e.g.* $[Ru(bpy)_2(bpyCOOH)](PF_6)_2$ (bpyCOOH = 3-carboxyl-2,2′-bipyridine).[10e] Since $[Ru(bpy)_2(hdppz)](ClO_4)_2$ in the protonated state is almost nonluminescent, made us impossible to accurately measure τ_{HB}, we have to use the second method, an approximate approach in which pK_a and pK_a* are related

Table 1 The comparisons of pK_a and pK_a* values and emission on/off ratios for $[Ru(bpy)_2(hdppz)]^{2+}$ with those previously reported for representative Ru(II) complexes

Complex[a]	pK_a	pK_a*	Emission on/off ratio (pH region)	Ref
$[Ru(bpy)_2(pidbH_2)]^{2+}$	1.97, 3.57, 10.56	4.22, 10.71	16 (0.6–12.0)	26*a*
$[(bpy)_2Ru(bpibH_2)Ru(bpy)_2]^{4+}$	4.11, 7.84	4.34, 7.46	2.5 (0–6.0); 4.0 (6.0–10.0)	26*b*
$[(bpy)_2Ru(ebipcH_2)Ru(bpy)_2]^{4+}$	4.16, 5.07, 9.65, 12.09	4.54, 5.07, 9.76, 12.09	100 (8.0–10.0)	16*a*
$[Ru(bpy)_2(ppi)]^{2+}$	8.8	9.1	3.0 (7.5–11.5)	16*e*
$[Ru(bpy)_2(Hbopip)]^{2+}$	1.70, 5.23, 8.22	3.06, 5.01, 8.22	20 (1.0–3.0); 3.0 (3.6–9.0)	16*b*
$[Ru(bpy)_2(hpbpy)]^{2+}$	8.6	8.6	~10 (6.5–10.5)	23*a*
$[Ru(bpy)_2dpq(OH)_2]^{2+}$	6.0, 10.0	6.5, 10.0	—	23*b*
$[Ru(bpy)_2(dpqOHCOOH)]^{2+}$	4.8, 6.4	5.5, 7.4	—	23*b*
$[Ru(bpy)_2(dhipH_3)]^{2+}$	2.1, 5.8, 8.7, 11.3	1.9, 6.3, 9.4, 12.3	20 (0.5–10.7)	16*d*
$[Ru(bpy)_2(hdppz)]^{2+}$	7.20–7.40	6.64–7.84	150 (6.0–11.5)	This work

[a] $pidbH_2$ = (1-[1,10]phenanthroline[5,6-*d*]imidazo-2-yl)-4-*N*,*N*-dimethylaminobenzene; $bpibH_2$ = 1,4-bis([1,10]phenanthroline[5,6-*d*]imidazo-2-yl)-benzene; $ebipcH_2$ = *N*-ethyl-4,7-bis([1,10]phenanthroline[5,6-*f*]imidazo-2-yl)carbazole); ppi = 2-pyridin-2-yl-1*H*-phenanthro[9,10-*d*]imidazole; Hbopip = 2-(4-benzoxazolyl)phenylimidazo[4,5-*f*][1,10]phenanthroline; hpbpy = 4-(4-hydroxyphenyl)-2,2′-bipyridine; $dpq(OH)_2$ = 2,3-dihydroxydipyrido[3,2-*f*:2′,3′-*h*]quinoxaline; dpqOHCOOH = 3-hydroxydipyrido[3,2-*f*:2′,3′-*h*]quinoxaline-2-carboxylic acid; $dhipH_3$ = 3,4-dihydroxy phenylimidazo[4,5-*f*][1,10]phenanthroline

thermodynamically by a Förster cycle.[27] The Förster treatment results in eqn (3), which describes the relationship between ground state pK_a and excited state pK_a* based on pure 0–0 transitions in wavenumbers of ν_B and ν_{HB} for the basic and acidic species, respectively.

$$pK_a^* = pK_a + (0.625/T)(\nu_B/\nu_{HB}) \quad (3)$$

In reality, the ν_B and ν_{HB} values are often difficult or even impossible to obtain. A good approximation is to use the emission maxima for ν_B and ν_{HB} since protonation equilibrium is almost certainly established between the ^{3}MLCT states. Therefore, the energies of the emission maxima in wavenumbers were used in eqn (3), and excited-state ionization constants of pK_a* = 7.64 and 7.84 were thus obtained for the complex at concentrations of 1.50 and 15.4 μM, respectively. The value of pK_a* is about 0.4 units greater than pK_a, indicating that the electron density was higher in the excited state than in the ground state for $[Ru(bpy)_2(hdppz)]^{2+}$, and the excited electron was directed on hdppz rather than bpy in $[Ru(bpy)_2(hdppz)]^{2+}$. The increase in electron density on the hdppz ligand increased its basicity and, therefore increased the excited-state pK_a* value.

3.3 DNA-binding properties

3.3.1 Thermal denaturation. Any type of weak interaction modifies, reversibly, the double helix structure, and the structural changes are reflected in measurable properties. The DNA thermal denaturation temperature is one of these.[28] Intercalation of small molecules into the double helix is known to increase the helix stability and thus the melting temperature, the temperature at which the double helix denatures into single-stranded DNA. The helix to coil transition temperature can be determined by monitoring the absorbance of the DNA bases at 260 nm as a function of temperature. Although the increase in denaturation temperature is not specific of any particular type of noncovalent interaction, ΔT_m values may give some indications on the binding mode. As shown in Fig. 3, in the absence of the Ru(II) complex, the T_m of ct-DNA was 61.3 °C, and was successively increased upon increasing the concentrations of $[Ru(bpy)_2(hdppz)](ClO_4)_2$. The melting point was increased approximately by 20 °C at a concentration ratio of [Ru] : [DNA] = 1 : 10. Table 2 compares ΔT_m, the increases of DNA melting temperature in the presence of selected complexes[28*a*,29–33] which bind to DNA in different binding modes. The large increase in ΔT_m suggests an intercalative binding of $[Ru(bpy)_2(hdppz)](ClO_4)_2$ to DNA. The DNA binding constant K of $[Ru(bpy)_2(hdppz)]^{2+}$ to ct-DNA at T_m were determined by McGee's equation.

$$1/T_m^0 - 1/T_m = (R/\Delta H_m)\ln(1 + KL)^{1/n} \quad (4)$$

Here T_m^0 is the melting temperature of ct-DNA alone, T_m is the melting temperature in presence of the complex, ΔH_m is the enthalpy of DNA melting, R is the gas constant, K is the DNA binding constant at T_m, L is the free Ru(II) complex concentration and n is the binding site size. K was derived to be 4.6×10^4 M^{-1} at 82 °C by taking n = 0.34 bp (obtained by UV-visible spectroscopy as will be discussed below) and ΔH_m = 6.9 kcal mol^{-1}, indicating that the complex still displayed a binding affinity at the melting point of DNA. This observation is similar to those for $[Ru(phen)_3]^{2+}$ and $[Ru(cyclam)(phi)]^{2+}$

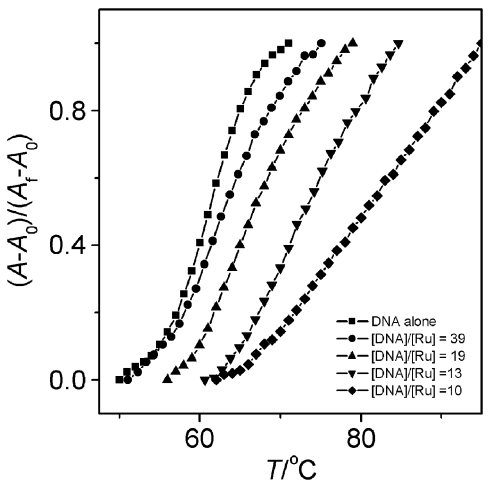

Fig. 3 Thermal denaturation curves of ct-DNA (60.0 μM) at varying concentration ratios of [Ru]/[DNA] in a buffer consisting of 1.5 mM Na_2HPO_4, 0.5 mM NaH_2PO_4 and 0.25 mM Na_2EDTA at pH = 6.8: [DNA]/[Ru] = 39 (–●–); 19 (–▲–); 13 (–▼–); 10 (–◆–) and DNA alone (–■–).

Table 2 The comparison of ΔT_m of ct-DNA upon the interaction with Ru(II) complexes

Complex[a]	$10^{-5}K_b/M^{-1}$ cm^{-1}	[DNA]/[Ru]	ΔT_m/°C	Ref
$[Ru(bpy)_3]^{2+}$	—	10	<2	29
$[Ru(phen)_3]^{2+}$	0.0055	12	18	29
EB	12.5	10	13	28*a*
$[Ru(phen)_2(dicnq)]^{2+}$	0.3	25	5	30
Δ-$[Ru(phen)_2(dppz)]^{2+}$	32	1	16	31
Λ-$[Ru(phen)_2(dppz)]^{2+}$	17	1	5	31
AMAC	0.2	1	5	33
$[Ru(bpy)_2(hdppz)]^{2+}$	1.3	10	20	This work

[a] bpy = 2,2′-Bipyridine; phen = phenanthroline; EB = ethidium bromide; dicnq = 6,7-dicyanodipyrido[2,2-*d*:2′,3′-*f*]quinoxaline; dppz = dipyrido[3,2-*a*:2′,3′-*c*]-phenazine; AMAC = (9-anthrylmethyl)ammonium chloride.

(cyclam = 1,4,8,11-tetraazacyclotetradecane, phi = 9,10-phenanthroquinonediimine),[29,32] but different from that of AMAC (AMAC = (9-anthrylmethyl)ammonium chloride).[33] The change of standard enthalpy was determined according to the van't Hoff's equation (eqn (5)),[8] and changes of standard free energy and standard entropy of the binding of the Ru(II) complex to DNA according to eqn (6) and (7).

$$\ln(K_1/K_2) = (\Delta H^0/R)[(T_1 - T_2)/T_1T_2] \quad (5)$$

$$\Delta G^0_T = -RT\ln K \quad (6)$$

$$\Delta G^0_T = \Delta H^0 - T\Delta S^0 \quad (7)$$

Here K_1 and K_2 are the DNA binding constants of the complex at temperature T_1 and T_2, respectively. ΔG^0_T, ΔH^0, and ΔS^0 are the changes of standard free energy, standard enthalpy, and standard entropy of binding of the complex to ct-DNA, respectively. A K_1 value of 1.3×10^5 M^{-1} (obtained by UV-visible spectroscopy as shown below, T_1 = 298 K) and a K_2 value of 4.6×10^4 M^{-1} (T_2 = 355 K) were used in eqn (5), ΔH^0 was thus derived to be −16.0 kJ mol^{-1}. By substituting K_1 = 1.3×10^5 M^{-1} (T_1 = 298 K) and ΔH^0 = −16.0 kJ mol^{-1} into eqn (6) and (7), $\Delta G^0_{298\ K}$ = −29.2 kJ mol^{-1} and ΔS^0 = 44.0 J mol^{-1} K^{-1} at 25 °C were derived. The negative binding free energy implies that the sum of the free energies of free complex and DNA are higher than the free energy of the adduct, and the binding of the Ru(II) complex to ct-DNA is energetically highly favorable at room temperature. However, the negative enthalpy change observed for $[Ru(bpy)_2(hdppz)](ClO_4)_2$, is in contrast to a positive one reported for $[Ru(phen)_2(dppz)]Cl_2$,[34*a*] but is similar to those observed for ethidium bromide[34*b*] and daunomycin.[34*c*] The positive entropy change could be a predominately hydrophobically driven binding reaction. Therefore the DNA binding reaction of $[Ru(bpy)_2(hdppz)](ClO_4)_2$ was both enthalpically and entropically driven.

3.3.2. Viscosity measurements. Optical photophysical probes provide necessary, but not sufficient, clues to support a binding model. Hydrodynamic measurements (*i.e.* viscosity and sedimentation) that are sensitive to the length changes of DNA are regarded as the least ambiguous and the most critical tests of a binding model in solution in the absence of crystallographic structural data.[8,35] A classical intercalation model results in lengthening the DNA helix as base pairs are separated to accommodate the binding ligand, leading to the increase of DNA viscosity. In contrast, drug molecules that bind exclusively in the DNA groove (*e.g.*, netropsin) under the same conditions, typically cause less pronounced or no change in DNA solution viscosity since they only produce subtle changes in the structure and the DNA remains essentially in an unperturbed B DNA form.[35] Fig. 4 shows the effects of successive additions of $[Ru(bpy)_2(hdppz)](ClO_4)_2$, $[Ru(bpy)_2(dppz)](ClO_4)_2$ and $[Ru(bpy)_3](ClO_4)$ on the viscosities of ct-DNA. The viscosities of the DNA increased dramatically upon addition of the complex which is similar to the behavior of the known DNA intercalator $[Ru(bpy)_2(dppz)](ClO_4)_2$.[36] On the contrary, for $[Ru(bpy)_3](ClO_4)_2$ which can not intercalate into the DNA, the viscosity values of the DNA remain almost constant upon addition of $[Ru(bpy)_3](ClO_4)_2$. The results strongly indicate that $[Ru(bpy)_2(hdppz)](ClO_4)_2$ intercalated into DNA base pairs deeply.

3.3.3. UV-visible spectra. The absorption spectra of $[Ru(bpy)_2(hdppz)](ClO_4)_2$ in the absence and the presence of ct-DNA are illustrated in Fig. 5(a). In the absence of the DNA, UV-visible spectra of the complex in 50 mM Tris–HCl buffer (pH 7.1, 50 mM NaCl) show that the lowest-energy MLCT transition absorption occurs at 443 nm, and the hdppz-centered intraligand (IL) π → π* band appeared at 372 nm, which is the same as those for

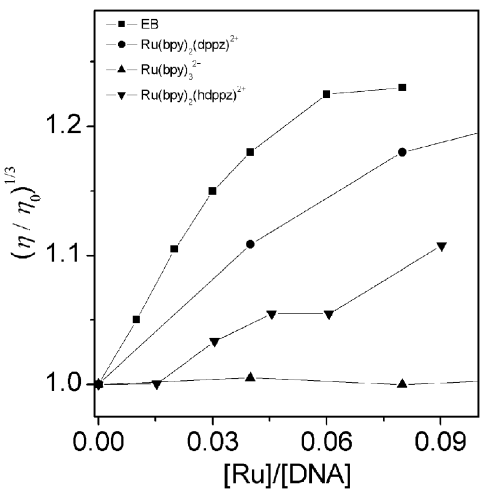

Fig. 4 The changes in relative viscosities of ct-DNA (0.450 mM) upon addition of $[Ru(bpy)_2(hdppz)](ClO_4)_2$ in 5 mM Tris–HCl buffer (pH 7.1, 50 mM NaCl): (–▼–); EB (–■–); $[Ru(bpy)_3](ClO_4)_2$ (–▲–); $[Ru(bpy)_2(dppz)](ClO_4)_2$ (–●–), shown as a function of the concentration ratios of [Ru]/[DNA].

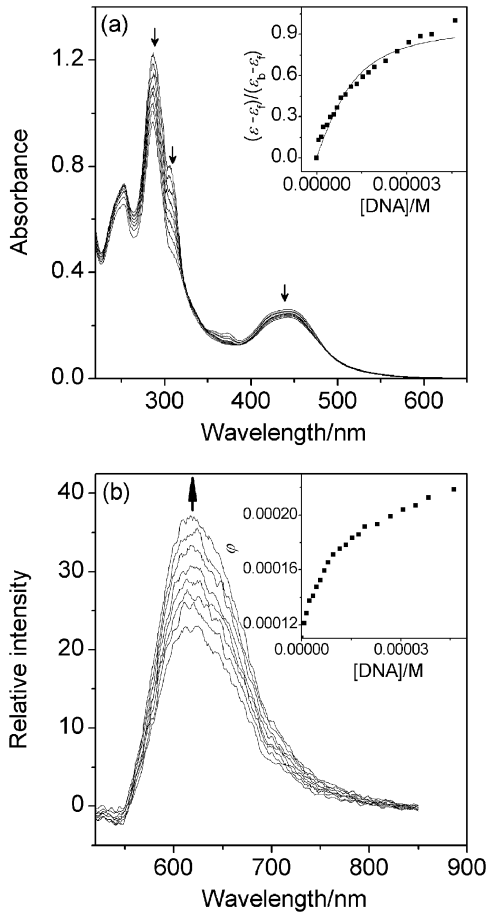

Fig. 5 The changes in UV-visible (a) and emission spectra (b) (λ_{ex} = 460 nm) of $[Ru(bpy)_2(hdppz)](ClO_4)_2$ (20.0 μM) with increasing concentrations of ct-DNA in 5 mM Tris–HCl buffer (pH 7.1, 50 mM NaCl). Arrows show spectral changes upon increasing DNA concentrations.

dppz and analogous complexes of $[Ru(bpy)_2(dppz)]^{2+}$ (372 nm), $[Ru(phen)_2(dppx)]^{2+}$ (372 nm, dppx = 4,5-dimethyldipyrido[3,2-*a*:2′,3′-*c*]phenazine) and $[Ru(phen)_2(dppm2)]^{2+}$ (372 nm, dppm2 = 6-methyldipyrido[3,2-*a*:2′,3′-*c*]phenazine),[5d] and is red-shifted with respect to the complex $[Ru(phen)_2(ndppz)]^{2+}$ (368 nm) with a $-NO_2$ substituted at the 6-position of phenazine ring.[18a] The decreased transition energies can also be observed in the following series: $[Ru(bpy)_2(dpatp)]^{2+}$ (dpatp = 4,5,9,18-tetraazaphenanthreno[9,10-*b*]triphenylene)[37a] (355 nm) > $[Ru(bpy)_2(hdppz)]^{2+}$ (372) ≈ $[Ru(phen)_2(phehat)]^{2+}$ (phehat = 1,10-phenanthrolino[5.6-*b*]-1,4,5,8,9,12-hexaazatriphenylene)[37b] (370 nm) > $[Ru(bpy)_2(tpphz)]^{2+}$ (tpphz = tetrapyrido[3,2-*a*:2′,3′-*c*:3″,2″-*h*:2‴,3‴-*j*]phenazine)[37c] (380 nm), suggesting enhanced conjugation on going from dpatp to tpphz. Considering the presence of self aggregation of $[Ru(bpy)_2(hdppz)]^{2+}$ in Tris–HCl buffer, different concentrations of $[Ru(bpy)_2(hdppz)](ClO_4)_2$ was used to specify the concentration-dependent DNA binding properties.

At a high concentration of the complex (20.0 μM) at which the complex is fully aggregated, all the absorption bands of the complex displayed clear hypochromicities and red shifts upon increasing concentrations of DNA (Fig. 5(a)). The hypochromism *H*%, as defined by $H\% = 100(A_{free} - A_{bound})/A_{free}$, for all the bands at 286, 306, 372 and 443 nm reached as high as 21, 40, 25 and 12% with almost no shift in the positions of the bands. The maximum hypochromism of 40% observed for the IL band at 306 nm, are larger than those observed for typical DNA intercalators: 32.1% (372 nm) for Δ-$[Ru(phen)_2(dppz)]^{2+}$ and 29.8% (372 nm) for Λ-$[Ru(phen)_2(dppz)]^{2+}$. At a low concentration of the complex (4.0 μM), the *H*% values were observed as being 20, 39, 26 and 10% for the bands at 286, 306, 372 and 443 nm, respectively, which are almost same as those observed at high concentration of the complex.

The intrinsic binding constant K_b illustrating the binding strength of the complex with ct-DNA, was determined from the eqn (8) and (9) through a plot of $(\varepsilon_a - \varepsilon_f)/(\varepsilon_b - \varepsilon_f)$ *vs.* [DNA], where [DNA] is the concentration of the DNA in nucleotides.

$$(\varepsilon_a - \varepsilon_f)/(\varepsilon_b - \varepsilon_f) = [b - (b^2 - 2K_b{}^2C_t[DNA]/s)^{1/2}]/(2K_bC_t) \quad (8)$$

$$b = 1 + K_bC_t + K_b[DNA]/2s \quad (9)$$

The apparent absorption coefficients ε_a, ε_f and ε_b correspond to A_{obsd}/[Ru], the extinction coefficient for the free ruthenium complex and the extinction coefficient for the ruthenium complex in the fully bound form, C_t is total Ru(II) complex concentration, and *s* is the binding site size.[38] The apparent DNA binding constant K_b and binding site size *s* of the complex with the DNA were derived to be $K_b = (1.3 \pm 0.3) \times 10^5\ M^{-1}$, $s = 0.3 \pm 0.1$ for the high concentration (20 μM) of $[Ru(bpy)_2(hdppz)](ClO_4)_2$ as shown from the inset in Fig. 5(a) by monitoring the decay of the absorbance at 305 nm, which are reasonable as comparison with $K_b = 4.4 \times 10^5\ M^{-1}$ ($s = 0.36$) reported for $[Ru(phen)_2(hdppz)](ClO_4)_2$ at [Ru] = 20 μM.[18a] It is noteworthy that the much larger K_b and *s* values of $K_b = (1.3 \pm 0.4) \times 10^6\ M^{-1}$, $s = 1.1 \pm 0.1$ for the low concentration (4 μM) of the complex were derived (Figure not shown). Although an equation which unifies self-aggregation constant and DNA binding constant K_b is required, in order to derive more accurate DNA binding constant K_D in the presence of evident self aggregation, the above results indeed indicate that the higher concentration of the complex has greater self-aggregating ability, greater competition with DNA binding, and resulting in a smaller DNA binding constant compared to the low concentration of the complex. As for the complex of $[Ru(bpy)_2(hdppz)]Cl_2$, the DNA binding constant and binding site size were derived to be $K_b = (1.6 \pm 0.5) \times 10^6\ M^{-1}$ and $s = 1.2 \pm 0.1$ for a high concentration (20 μM) of the complex, and $K_b = (5.6 \pm 1.1) \times 10^6\ M^{-1}$ and $s = 2.2 \pm 0.1$ for a low concentration (4 μM) of the complex, as shown in ESI.† The difference in DNA binding constants derived at higher and lower complex concentrations for $[Ru(bpy)_2(hdppz)]Cl_2$ is much less than those for $[Ru(bpy)_2(hdppz)](ClO_4)_2$, which is consistent with greater aggregation ability of $[Ru(bpy)_2(hdppz)](ClO_4)_2$ than $[Ru(bpy)_2(hdppz)]Cl_2$ as observed by UV-visible spectroscopy. Obviously, aggregates of $[Ru(bpy)_2(hdppz)]^{2+}$ require a suitable counter ion to stabilize. An apparent DNA binding constant of $K_b = (1.3 \pm 0.3) \times 10^5\ M^{-1}$ derived at high $[Ru(bpy)_2(hdppz)](ClO_4)_2$ concentration, is much lower than

expected from absence of self-aggregation, is much lower than those reported for strong DNA intercalators of Λ-[Ru(phen)$_2$(dppz)]$^{2+}$ (1.7×10^6 M^{-1}),[39] and of ethidium bromide (1.25×10^6 M^{-1}),[40] but is still a reasonable value for a DNA intercalator as comparison with K_b values reported for DNA intercalators: $K_b = 2.1 \times 10^4$ M^{-1} for [Ru(bpy)$_2$(DDT)]$^{2+}$ (DPT = 3-(pyrazin-2-yl)-*as*-triazino[5,6-*f*]phenanthrene),[36] $K_b = 1.7 \times 10^5$ M^{-1} for [Ru(bpy)$_2$(TAPTP)]$^{2+}$ (TAPTP = 4,5,9,18-tetraazaphenthreno[9,10-*b*]triphenylene),[37a] and 4.4×10^5 M^{-1}derived for [Ru(phen)$_2$(hdppz)](ClO$_4$)$_2$ at [Ru] = 20 μM.[18a] The above results may strongly suggest that the complex most likely intercalatively bound to DNA, involving a strong π–π stacking interaction between the aromatic chromophore and the base pairs of the DNA. Additionally, Chaires and Nordén[34a] explained that a value of $s < 1$ indicates that some intercalator molecules are stacking with each other on the surface. A value of $s < 1$ obtained for [Ru(bpy)$_2$(hdppz)](ClO$_4$)$_2$ at [Ru] = 20 μM, may be due to the fact that the aggregates formed by π–π stacking aromatic chromophores or intermolecular H-bonding interaction of [Ru(bpy)$_2$(hdppz)]$^{2+}$ on the DNA surface, dissociate into monomers followed by binding intercalatively to the DNA.

3.3.4. Luminescence studies. The complex in aerated aqueous solutions at room temperature emits weakly with luminescence peak at 609 nm which is red-shifted relative to [Ru(phen)$_2$(hdppz)](ClO$_4$)$_2$ (591 nm).[18a] The changes in emission spectra of the complex at concentrations of 20.0 μM with increasing DNA concentrations are shown in Fig. 5(b). As the DNA was successively added into the complex solution, the emission intensities of the complex were gradually increased. Similar changes have been observed for the complex at concentrations of 4.0 μM. Enhancements are normally observed for complexes bearing extended aromatic planar ligand binding to DNA,[41] since the hydrophobic environment inside the DNA helix reduces the accessibility of water molecules to the complex and the complex mobility is restricted at the binding site, leading to a decrease of the vibrational modes of relaxation.[37a]

Steady-state emission quenching experiments using [Fe(CN)$_6$]$^{4-}$ as the quencher also supported the intercalative binding proposal. As shown in Fig. 6, the emission of the complex was efficiently quenched by [Fe(CN)$_6$]$^{4-}$ in the absence of DNA, resulting in a strictly linear Stern–Volmer plot with slopes of 1.6 and 1.4 mM^{-1} for a low and a high ruthenium complex concentrations of 3.0 and 25.0 μM, respectively. The above difference in slopes at [Ru] = 3.0 and 25.0 μM may arise from different degrees of ion pairing between the Ru(II) complex cation and highly charged [Fe(CN)$_6$]$^{4-}$ at high concentrations, and of self-aggregation of the Ru(II) complex cation. These slopes are close to the slope of 2.2 mM^{-1} for [Ru(bpy)$_2$(ip)]$^{2+}$ and 2.0 mM^{-1} for [Ru(bpy)$_2$(pip)]$^{2+}$.[42] However, addition of DNA made the slopes decrease. This behavior may be explained by the repulsion of the highly anionic [Fe(CN)$_6$]$^{4-}$ by the DNA polyanion which hinders the bound complex from quenching of the emission. The slopes obtained under similar experimental condition, could reflect different degrees of protection or

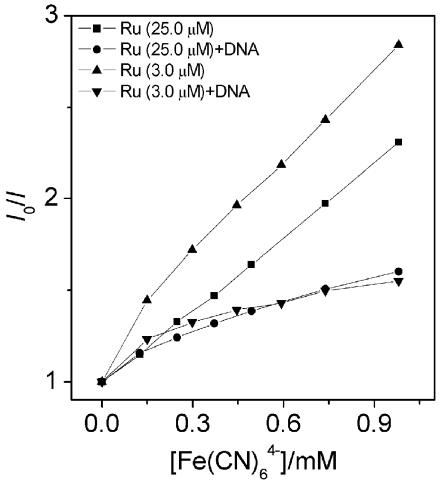

Fig. 6 Emission quenching curves of [Ru(bpy)$_2$(hdppz)](ClO$_4$)$_2$ with increasing concentrations of [Fe(CN)$_6$]$^{4-}$ (0.0–1.0 mM) in the absence and the presence of ct-DNA in 5 mM Tris–HCl buffer (pH 7.1, 50 mM NaCl). [Ru(bpy)$_2$(hdppz)]$^{2+}$ (3.0 μM) (–▲–); [Ru(bpy)$_2$(hdppz)]$^{2+}$ (3.0 μM) + DNA (–▼–); [Ru(bpy)$_2$(hdppz)]$^{2+}$ (25.0 μM) (–■–); [Ru(bpy)$_2$(hdppz)]$^{2+}$ (25.0 μM) + DNA (–●–).

relative accessibility of bound cations, and could be taken as a measure of binding affinity.

The competitive binding experiments[43] with a well-established quenching assay based on the displacement of the intercalating drug EB from ct-DNA may give further information regarding the DNA binding properties of the complex to DNA. If the complex were a DNA intercalator, the addition of the complex to DNA, pretreated with EB caused the removal of EB molecules inserted between the base pairs, and the free EB molecules were much less fluorescent than the bound EB molecules because of the surrounding water molecules which would quench the fluorescence. As shown in Fig. 7, the addition of [Ru(bpy)$_2$(hdppz)](ClO$_4$)$_2$ to the EB–DNA system resulted in appreciable reduction in emission intensity by 92%

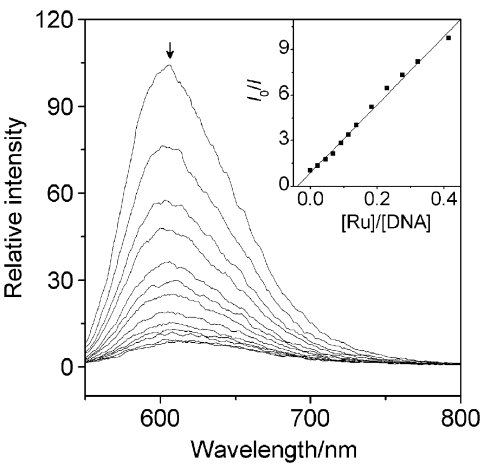

Fig. 7 Emission spectra of EB bound to DNA in the presence of [Ru(bpy)$_2$(hdppz)](ClO$_4$)$_2$ (0.0–60.0 μM) in 5 mM Tris–HCl buffer (pH 7.1, 50 mM NaCl). The arrows show the intensity changes upon increasing concentrations of the complex. Inset: fluorescence quenching curve of DNA-bound EB by the complex: [DNA] = 100.0 μM, [EB] = 20.0 μM, λ_{ex} = 537 nm.

relative to that observed in the absence of the complex, supporting the intercalative binding of the complex to the DNA. The quenching plot of I_0/I *vs.* [Ru]/[DNA] (the inset of Fig. 7) was in good agreement with the linear Stern–Volmer equation with a slope of 22.5. The results are also consistent with an intercalative binding mode, since groove DNA binders were reported to be also capable of causing the reduction in EB emission intensities, but only moderately.[44]

4 Conclusions

The complexes of $[Ru(bpy)_2(hdppz)]X_2$ (X = ClO_4^-, PF_6^- and Cl^-) have been evidenced that their ion association properties are strongly dependent on the counter ions and concentrations. The ion association moderately affects the ground- and excited-state acid–base properties of the complex, as characterized by the ground- and excited-state ionization constants of $pK_a = 7.20$ and $pK_a^* = 7.64$ derived at the low concentration of the complex, and $pK_a = 7.40$ and $pK_a^* = 7.84$ at the high concentration of the complex, respectively. More importantly, the ion association of the complex strongly affects DNA binding affinities of the complex, resulting in the DNA binding constant derived at the high concentration of the complex, is one order of magnitude smaller than that obtained at the low concentration of the complex. Therefore, this study has provided insight into a fundamental but important issue that should be taken into account for the DNA binding studies. The pH spectrophotometric titrations of the complex showed that both UV-visible and emission spectra of the complex are quite pH dependent, and the complex was demonstrated to be an interesting pH-induced emission switch with a large on–off ratio of ~150 over pH range 6.00–11.50. The results of UV-visible and luminescence titrations, steady-state emission quenching by $[Fe(CN)_6]^{4-}$, DNA competitive binding with ethidium bromide, and DNA melting experiments are all consistent with a DNA intercalative binding mode. The further applications of the complex in pH-modulated biological functionalities and fluorescent switching devices are in progress.

Acknowledgements

The authors wish to thank NSFC (90401007 and 20771016), Beijing Natural Science Foundation (2072011) and SRFDP (20060027002) for financial support.

References

1 (*a*) K. Rurack and U. Resch-Genger, *Chem. Soc. Rev.*, 2002, 116; (*b*) J. J. Lavigne and E. V. Anslyn, *Angew. Chem., Int. Ed.*, 2001, **40**, 3119; (*c*) V. Amendola, L. Fabbrizzi, C. Mangano and P. Pallavicini, *Acc. Chem. Res.*, 2001, **34**, 488; (*d*) A. W. Czarnik, *Acc. Chem. Res.*, 1994, **27**, 302; (*e*) L. Fabbrizzi, M. Licchelli and P. Pallavicini, *Acc. Chem. Res.*, 1999, **32**, 846; (*f*) F. M. Raymo, *Adv. Mater.*, 2002, **14**, 401; (*g*) F. M. Raymo and S. Giordani, *J. Am. Chem. Soc.*, 2002, **124**, 2004; (*h*) A. P. de Silva, H. Q. N. Gunaratue, T. Gunnlaugsson, A. J. M. Huxley, C. P. McCoy, J. T. Rademacher and T. E. Rice, *Chem. Rev.*, 1997, **97**, 1515.

2 (*a*) A. Juris, V. Balzani, F. Barigelleti, S. Campagna, P. Belsar and A. von Zelewsky, *Coord. Chem. Rev.*, 1988, **84**, 85; (*b*) J. N. Demas and B. A DeGraff, *Anal. Chem.*, 1991, **63**, 829.

3 (*a*) J. C. Chambron, J. P. Sauvage, E. Amouyal and P. Koffi, *New J. Chem.*, 1985, **9**, 527; (*b*) E. Amouyla, A. Homsi, J. C. Chambron and J. P. Sauvage, *J. Chem. Soc., Dalton Trans.*, 1990, 1841; (*c*) J. Fees, W. Kaim, M. Moscherosch, W. Matheis, J. Klima, M. Krejcik and S. Zalis, *Inorg. Chem.*, 1993, **32**, 166; (*d*) J. R. Schoonover, W. D. Bates and T. J. Meyer, *Inorg. Chem.*, 1995, **34**, 6421.

4 E. R. Batista and R. L. Martin, *J. Phys. Chem. A*, 2005, **109**, 3128.

5 (*a*) Y. Jenkins, A. E. Friedman, N. J. Turro and J. K. Barton, *Biochemistry*, 1992, **31**, 10809; (*b*) E. Sabatani, H. D. Nikol, H. B. Gray and F. C. Anson, *J. Am. Chem. Soc.*, 1996, **118**, 1158; (*c*) A. E. Friedman, J. C. Chambron, J. P. Sauvage, N. J. Turro and J. K. Barton, *J. Am. Chem. Soc.*, 1990, **112**, 4960; (*d*) R. M. Hartshorn and J. K. Barton, *J. Am. Chem. Soc.*, 1992, **114**, 5919; (*e*) C. M. Dupureur and J. K. Barton, *J. Am. Chem. Soc.*, 1994, **116**, 10286.

6 (*a*) C. Turro, S. H. Bossmann, Y. Jenkins, J. K. Barton and N. Turro, *J. Am. Chem. Soc.*, 1995, **117**, 9026; (*b*) M. K. Brennaman, T. J. Meyer and J. M. Papanikolas, *J. Phys. Chem. A*, 2004, **108**, 9938.

7 H. Xu, K. C. Zheng, Y. Chen, Y. Z. Li, L. J. Lin, H. Li, P. X. Zhang and L. N. Ji, *Dalton Trans.*, 2003, 2260, and references therein.

8 S. Satyanarayana, J. C. Dabrowiak and J. B. Chaires, *Biochemistry*, 1992, **31**, 9319.

9 (*a*) J. G. Liu, Q. L. Zhang, X. F. Shi and L. N. Ji, *Inorg. Chem.*, 2001, **40**, 5045; (*b*) X. H. Zou, B. H. Ye, H. Li, J. G. Liu, Y. Xiong and L. N. Ji, *J. Chem. Soc., Dalton Trans.*, 1999, 1423.

10 (*a*) J. G. Vos, *Polyhedron*, 1992, **11**, 2285; (*b*) F. Casalboni, Q. G. Mulazzani, C. D. Clark, M. Z. Hoffman, P. Orizondo, M. Perkovic and D. P. Rillema, *Inorg. Chem.*, 1997, **36**, 2252; (*c*) M. A. Haga, T. Ano, K. Kano and S. Yamabe, *Inorg. Chem.*, 1991, **30**, 3843; (*d*) V. W. W. Yam and A. S. F. Kai, *Inorg. Chim. Acta*, 2000, **300–302**, 82; (*e*) G. Y. Zheng, Y. Wang and D. P. Rillema, *Inorg. Chem.*, 1996, **35**, 7118; (*f*) M. A. Haga, T. Ano, T. Ishizaki, K. Kano, K. Nozaki and T. Ohno, *J. Chem. Soc., Dalton Trans.*, 1994, 263; (*g*) M. A. Haga, T. Takasugi, A. Tomie, M. Ishizuya, T. Yamada, M. D. Hossain and M. Inoue, *Dalton Trans.*, 2003, 2069.

11 (*a*) L. Fabbrizzi, F. Gatti, P. Pallavicini and L. Parodi, *New J. Chem.*, 1998, 1403; (*b*) C. S. Allardyce, P. J. Dyson, D. J. Ellis and S. L. Heath, *Chem. Commun.*, 2001, 1396.

12 (*a*) P. J. Barnard and R. S. Vagg, *J. Inorg. Biochem.*, 2005, **99**, 1009; (*b*) Y. Masuda and H. Yamatera, *Bull. Chem. Soc. Jpn.*, 1984, **57**, 58; (*c*) J. R. Aldrich-Wright, R. S. Vagg and P. A. Williams, *Coord. Chem. Rev.*, 1997, **166**, 361; (*d*) E. M. Proudfoot, J. P. Mackay and P. Karuso, *Dalton Trans.*, 2003, 165; (*e*) S. D. Bergman, *M. Kol. Inorg. Chem.*, 2005, **44**, 1647; (*f*) A. K. Bilakhiya, B. Tyagi and P. Parimal, *Inorg. Chem.*, 2002, **41**, 3830; (*g*) A. Rudi, Y. Kashman, D. Gut, F. Lellouche and M. Kol, *Chem. Commun.*, 1997, 17; (*h*) D. Gut, A. Rudi, J. Kopilov, I. Goldberg and M. Kol, *J. Am. Chem. Soc.*, 2002, **124**, 5449; (*i*) R. Caspar, L. Musatkina, A. Tatosyan, H. Amouri, M. Gruselle, C. Guyard-Duhayon, R. Duval and C. Cordier, *Inorg. Chem.*, 2004, **43**, 7986.

13 (*a*) We appreciate one of the reviewers who pointed out the possibility of ion pairing; (*b*) M. Alceo, *Chem. Rev.*, 2005, **105**, 2039; (*c*) Y. Marcus and G. Hefter, *Chem. Rev.*, 2006, **106**, 4585.

14 (*a*) Z. Daniele, B. Gianfranco, C. Giuseppe, C. Gianluca and Z. Cristiano, *Organometallics*, 2007, **26**, 3930; (*b*) D. Zuccaccia, E. Foresti, S. Pettirossi and P. Sabatino, *Organometallics*, 2007, **26**, 6099.

15 (*a*) C. Isabelle, A. Hani and C. Christine, *Organometallics*, 2007, **26**, 1150; (*b*) D. Zuccaccia, S. Sabatini, G. Bellachioma, G. Cardaci, E. Clot and A. Macchioni, *Inorg. Chem.*, 2003, **42**, 5465; (*c*) N. C. Fletcher and F. R. Keene, *J. Chem. Soc., Dalton Trans.*, 1999, 683; (*d*) R. Caspar, H. Amouri, M. Gruselle, C. Cordier, B. Malézieux, R. Duval and H. Lévéque, *Eur. J. Inorg. Chem.*, 2003, 499.

16 (*a*) F. R. Liu, K. Z. Wang, G. Y. Bai, Y. A. Zhang and L. H. Gao, *Inorg. Chem.*, 2004, **43**, 1799; (*b*) M. J. Han, L. H. Gao, Y. Y. Lü and K. Z. Wang, *J. Phys. Chem. B*, 2006, **110**, 2364; (*c*) M. J. Han, Z. M. Duan, Q. Hao, S. Z. Zheng and K. Z. Wang, *J. Phys. Chem. C*, 2007, **111**, 16577; (*d*) G. Y. Bai, K. Z. Wang, Z. M. Duan and L. H. Gao, *J. Inorg. Biochem.*, 2004, **98**, 1017;

(*e*) K. Z. Wang, L. H. Gao, G. Y. Bai and L. P. Jin, *Inorg. Chem. Commun*., 2002, **5**, 841; (*f*) M. J. Han, L. H. Gao and K. Z. Wang, *New J. Chem*., 2006, **30**, 208; (*g*) Y. Y. Lü, L. H. Gao, M. J. Han and K. Z. Wang, *Eur. J. Inorg. Chem*., 2006, 430; (*h*) B. Y. Wu, L. H. Gao, Z. M. Duan and K. Z. Wang, *J. Inorg. Biochem*., 2005, **99**, 1685; (*i*) Q. Hao, Z. M. Duan, M. J. Han, S. Z. Zheng and K. Z. Wang, *Chem. J. Chinese Univ*., 2006, **27**, 1217 (in Chinese); (*j*) J. Nie, M. J. Han and K. Z. Wang, *Chem. J. Chinese Univ*., 2007, **28**, 1833 (in Chinese).

17 R. B. Nair, B. M. Cullum and C. J. Murphy, *Inorg. Chem*., 1997, **36**, 962.

18 (*a*) X. W. Liu, J. Li, H. Li, K. C. Zheng, H. Chao and L. N. Ji, *J. Inorg. Biochem*., 2005, **99**, 2372; (*b*) C. Hiort, P. Lincoln and B. Norden, *J. Am. Chem. Soc*., 1993, **115**, 3448.

19 B. P. Sullivan, D. J. Salmon and T. J. Meyer, *Inorg. Chem*., 1978, **17**, 3334.

20 (*a*) H. Chao, B. H. Ye, Q. L. Zhang and L. N. Ji, *Inorg. Chem. Commun*., 1999, **2**, 338; (*b*) L. F. Tan, S. Zhang, H. Chao, K. C. Zheng, F. Wang, Y. Xiao and L. N. Ji, *Helv. Chim. Acta*, 2007, **90**, 1786; (*c*) J. M. Kim, J. M. Lee, J. Y. Choi, H. M. Lee and S. K. Kim, *J. Inorg. Biochem*., 2007, **101**, 1386; (*d*) S. E. Evans, A. Grigoryan and V. A. Szalai, *Inorg. Chem*., 2007, **46**, 8349; (*e*) L. F. Tan, H. Chao, Y. F. Zhou and L. N. Ji, *Polyhedron*, 2007, **26**, 3029; (*f*) L. Bouffier, M. Demeunynck, P. Dumy, C. Moucheron and M. A. Kirsch-De, *Inorg. Chim. Acta*, 2007, **360**, 3162.

21 R. Margalit, N. Shaklai and S. Cohen, *Biochem. J*., 1983, **209**, 547.

22 P. J. Giordano, C. R. Bock and M. S. Wrighton, *J. Am. Chem. Soc*., 1978, **100**, 6960.

23 (*a*) A. M. W. C. Thompson, M. C. C. Smailes, J. C. Jeffery and M. D. Ward, *J. Chem. Soc., Dalton Trans*., 1997, 737; (*b*) B. Gholamkhass, K. Koike, N. Negishi, H. Hori and K. Takeuchi, *Inorg. Chem*., 2001, **40**, 756.

24 L. C. Xu, J. Li, Y. Shen, K. C. Zheng and L. N. Ji, *J. Phys. Chem. A*, 2007, **111**, 273.

25 R. Grigg and W. D. J. A. Borbert, *J. Chem. Soc., Chem. Commun*., 1992, 1300.

26 (*a*) B. W. Jing, T. Wu, C. H. Tai, M. H. Zhang and T. Shen, *Bull. Chem. Soc. Jpn*., 2000, **73**, 1749; (*b*) H. Cao, B. H. Ye, H. Li, R. H. Li, J. Y. Zhou and L. N. Ji, *Polyhedron*, 2000, **19**, 1975.

27 E. V. Donckt, in *Process in Reaction Kinetics*, ed. G. Poter, Pergamon Press, Oxford, UK, 5th edn, 1970.

28 (*a*) M. Cory, D. D. Mckee, J. Kagan, D. W. Henry and J. A. Miller, *J. Am. Chem. Soc*., 1985, **107**, 2528; (*b*) P. U. Maheswari and M. Palaniandavar, *J. Inorg. Biochem*., 2004, **98**, 219; (*c*) S. Satyanarayana, J. C. Dabrowiak and J. B. Chaires, *Biochemistry*, 1993, **32**, 2573.

29 J. M. Kelly, A. B. Tossi, D. J. McConnell and C. OhUigin, *Nucleic Acids Res*., 1985, **13**, 6017.

30 A. Ambroise and B. G. Maiya, *Inorg. Chem*., 2000, **39** 4264.

31 C. M. Dupureur and J. K. Barton, *Inorg. Chem*., 1997, **36** 33.

32 H. L. Chan, H. Q. Liu, B. C. Tzeng, Y. S. You, S. M. Peng, M. Yang and C. M. Che, *Inorg. Chem*., 2002, **41**, 3161.

33 C. V. Kumar and E. H. Asuncion, *J. Am. Chem. Soc*., 1993, **115**, 8547.

34 (*a*) I. Haq, P. Lincoln, D. Suh, B. Nordén, B. Z. Chowdhry and J. B. Chaires, *J. Am. Chem. Soc*., 1995, **117**, 4788; (*b*) H. P. Hopkins, J. Fumero and W. D. Wilson, *Biopolymers*, 1990, **29**, 445; (*c*) J. B. Chkres, W. Priebe, D. E. Graves and T. G. Burke, *J. Am. Chem. Soc*., 1993, **115**, 5360.

35 L. Lerman, *J. Mol. Biol*., 1961, **3**, 18.

36 H. Deng, J. Cai, H. Xu, H. Zhang and L. N. Ji, *Dalton Trans*., 2003, 325.

37 (*a*) Q. X. Zhen, B. H. Ye, Q. L. Zhang, J. G. Liu, H. Li, L. N. Ji and L. Wang, *J. Inorg. Biochem*., 1999, **76**, 47; (*b*) L. Julien, E. Benjamin, M. Cecile and K-D. M. Andree, *Inorg. Chem*., 2005, **44**, 393; (*c*) J. Bolger, A. Gourdon, E. Ishow and J. Launay, *Inorg. Chem*., 1996, **35**, 2937.

38 R. B. Nair, E. S. Teng, S. L. Kirkland and C. J. Murphy, *Inorg. Chem*., 1998, **37**, 139.

39 J. B. Lepeep and C. Paoletti, *J. Mol. Biol*., 1967, **27**, 87.

40 M. J. Waring, *J. Mol. Biol*., 1965, **13**, 269.

41 Q. X. Zhen, Q. L. Zhang, J. G. Liu, B. H. Ye, L. N. Ji and L. Wang, *J. Inorg. Biochem*., 2000, **78**, 293.

42 Y. Xiong, X. F. He, X. H. Zou, J. Z. Wu, X. M. Chen, L. N. Ji, R. H. Li, J. Y. Zhou and K. B. Yu, *J. Chem. Soc., Dalton Trans*., 1999, 19.

43 (*a*) I. Ortmans, B. Elias, J. M. Kelly, C. Moucheron and A. K. Demesmaeker, *Dalton Trans*., 2004, 668; (*b*) W. C. Tse and D. L. Boger, *Acc. Chem. Res*., 2004, **37**, 61.

44 D. L. Boger, B. E. Fink, S. R. Brunette, W. C. Tse and M. P. Hedrick, *J. Am. Chem. Soc*., 2001, **123**, 5878.

